Search for regular orbits in the x^2y^2 potential problem

1992 J. Phys. A: Math. Gen. 25 5553

(http://iopscience.iop.org/0305-4470/25/21/014)

J. Phys. A: Math. Gen. 25 (1992) 5553-5562. Printed in the UK

Search for regular orbits in the x^2y^2 potential problem

M L A Nip†, J A Tuszyński†, M Otwinowski† and J M Dixon‡

† Department of Physics, University of Alberta, Edmonton, Alberta, T6G 2J1, Canada
‡ Department of Physics, University of Warwick, Coventry CV4 7AL, UK

Received 27 January 1992, in final form 25 June 1992

Abstract. Analytical and numerical investigation is provided into the motion of a particle close to unstable straight-interval $y \approx \pm x$ orbits in the system $H = \frac{1}{2}(p_x^2 + p_y^2 + x^2y^2)$. Physical interpretation is provided which involves a perturbation analysis leading to doubly periodic solutions for $x(t)$ and $y(t)$. Second-order ordinary differential equations are derived to describe the trajectory of the particle in the x-y plane and the functional form of $x(t)$.

1. Introduction

The classical Hamiltonian

$$H = \tfrac{1}{2}(p_x^2 + p_y^2 + x^2y^2) \tag{1}$$

has been the subject of numerous studies (see Dahlqvist and Russberg 1990 and references therein). The practical importance of the problem under investigation rests chiefly with its relationship to the plasma confinement problem. In this regard, the Hamiltonian in equation (1) arises from a three-dimensional Hamilitonian for a charged particle of mass m in the presence of a magnetic vector potential $\boldsymbol{A}$. The Hamiltonian for this case is

$$H = \frac{1}{2m}\left\{p_x^2 + p_y^2 + \left(p_z - \frac{eA}{c}\right)^2\right\} \tag{2}$$

where the vector potential is taken as $\boldsymbol{A} = xy\boldsymbol{k}$, with $\boldsymbol{k}$ being a unit vector along the z-axis. Our Hamiltonian of equation (1) arises by restricting the motion to the x-y plane when $p_z = 0$. The gauge used corresponds to a magnetic induction field $\boldsymbol{B}$ of the form

$$\boldsymbol{B} = x\boldsymbol{i} - y\boldsymbol{j} \tag{3}$$

the magnitude of $\boldsymbol{B}$ being proportional to the radius $r = (x^2 + y^2)^{1/2}$.

An important physical application of the Hamiltonian in equation (1) is in the context of classical approximations to the Yang-Mills gauge field theory. A particular point of interest is the effect of the ground state in quantum chromodynamics (Matanyan *et al* 1981, Chirikov and Shepelyonsky 1981, Nikolaevskii and Shur 1982, Savvidy 1983, 1984, Carnegie and Percival 1984, Chang 1984, Steeb *et al* 1985, Sohos *et al* 1989). It was conjectured that the system described by equation (1) is simultaneously globally ergodic and given by an analytical expression (Martens *et al* 1989). This Hamiltonian has also been used to test the conjecture that if a quantum system has a classically chaotic analogue then, in the semi-classical limit, the energy eigenfunctions

0305-4470/92/215553+10$07.50

fill the entire accessible phase space (Feingold *et al* 1985). For this example to be appropriate all the periodic orbits must be unstable. However, very recently Dahlqvist and Russberg (1990) provided evidence for the existence of stable periodic orbits and disproved this claim. This one-parameter family of stable orbits occupies an area of 0.005% on the surface of the section and this explains why it was so difficult to find it. Furthermore a recent communication by Biswas *et al* (1992) has claimed the presence of another stable family of periodic orbits and these two discoveries tend to rule out ergodicity in this class of Hamiltonian systems. Assuming for simplicity that $\dot{x}(0) = \dot{y}(0) = 0$, we believe we have found a periodic orbit, shown in figure 1 for illustrative purposes, which very closely resembles the one discussed by Dahlqvist and Russberg (1990). Although this may only be a numerical inaccuracy our computations tend to indicate that over several periods of time this orbit appears to become open. The objective of the present paper, however, is not to discuss the stability of this or other periodic orbits, but rather the behaviour of particle motion close to the unstable straight-line trajectories $y = \pm x$. This is in order to gain some insight into particle motion close to instabilities. In particular, we shall investigate whether a combination of analytical and numerical methods can explain the observed distortion of straight-line trajectories into periodic or quasi-periodic orbits.

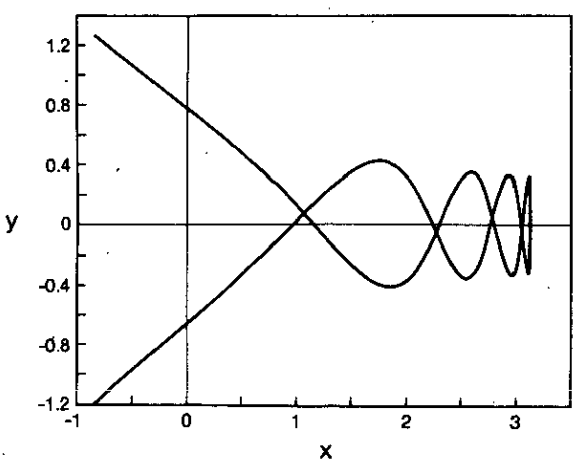

Figure 1. A plot of y versus x for the periodic orbit corresponding to $x_0 = -0.800\,54$ and $E = 0.5$.

2. The $y = \mp x$ oribits and their neighbourhood

In this paper we point out the importance of two straight-interval orbits $y = \mp x$ which yield analytical solutions to the equations of motion

$$\ddot{x} = -xy^2 \qquad \ddot{y} = -yx^2. \tag{4}$$

These solutions are given by

$$x(t) = (2E)^{1/4}\,\mathrm{cn}[(2E)^{1/4}t, 1/\sqrt{2}] \tag{5}$$

where E is the total energy and cn is a Jacobi elliptic function (Byrd and Friedman 1971) whose modulus is $k = 1/\sqrt{2}$. Thus, its amplitude scales with $(2E)^{1/4}$ and its period T is

$$T = 4K(1/\sqrt{2})/(2E)^{1/4} \tag{6}$$

where K denotes the complete elliptic integral of the first kind. In this case $K(1/\sqrt{2}) = 1.854\,075$ (Byrd and Friedman 1971). These orbits appear to be unstable with respect to the initial conditions but, as shown in figures 2(a–c), under small perturbation of the initial conditions they can be transformed into what appear to be quasi-periodic orbits. Changing the initial conditions ($x_0 = x(t)$ at $t = 0$) by an infinitesimally small amount, either above or below $x_0 = -1$, results in a new solution which initially follows a straight-line trajectory fairly closely and then, for the value of y close to zero, departs from it, changing the direction of propagation to along the y-axis or along the x-axis

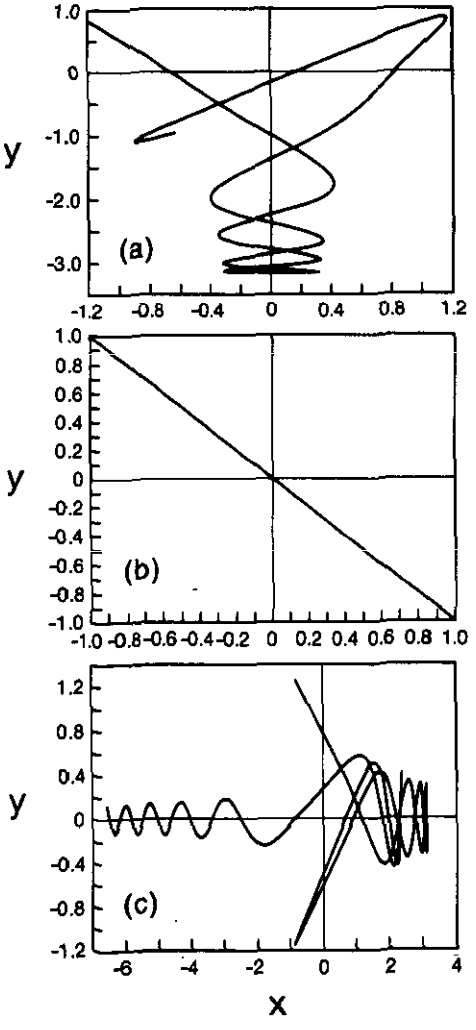

Figure 2. Trajectories in the x–y plane for $E = 0.5$ and (a) $x_0 = -1.2$, (b) $x_0 = -1.0$, (c) $x_0 = -0.8$.

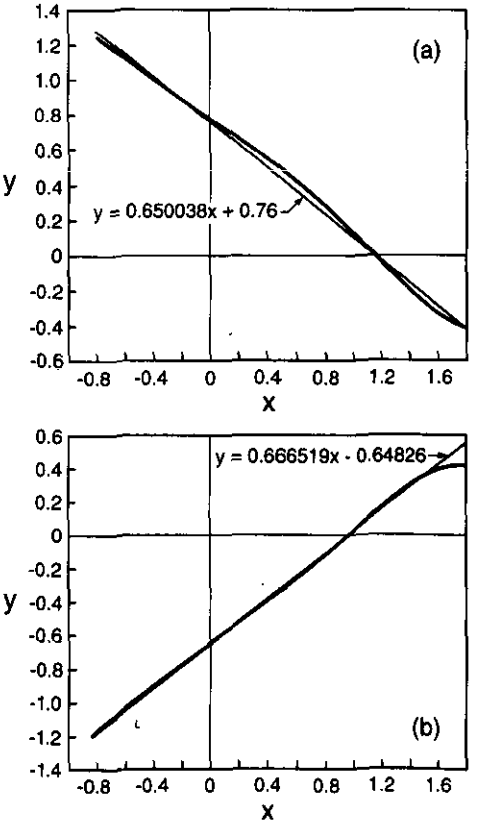

Figure 3. Best-fit plots for equations (9) and (10) in panels (a) and (b), respectively.

depending on initial conditions. This behaviour can be readily understood in terms of the potential function illustrated in figure 4(a), and especially from the contour plot in figure 4(b) which shows that the two axes point in the direction of the potential's troughs. The original straight-line trajectories represent unstable solutions traversing the locus of points representing local potential energy maxima. An infinitesimally small perturbation will have a tendency to cause the trajectory to deviate from its straight-line path and seek the most energetically favourable course. This obviously means a redirection of the motion along either the x or y axes, where the potential energy is lowest and the walls surrounding it are steepest and become closer together with increasing x or y, respectively. Furthermore, it can be seen that, apart from the initial and final points of a quasi-periodic orbit, the particle's trajectory never makes contact with the constant potential energy hyperbolae. This is due to the fact that initially the kinetic energy is assumed to be zero (i.e. $\dot{x}(0)=\dot{y}(0)=0$) and, as energy is conserved, only classical turning points will have the same potential energy as the initial point.

Obviously, assuming a different set of initial conditions especially with a non-zero kinetic energy will affect the final result. In particular, the direction of propagation will depend directly on the values of $\dot{x}(0)$ and $\dot{y}(0)$ since the initial angle of entry is given by $\tan\theta=(p_y/p_x)|_{t=0}$. However, the straight-line $y=\pm x$ orbits can be recovered by putting $x_0=\pm y_0$ and $\dot{x}(0)=\pm\dot{y}(0)$.

Note that there is another pair of straight-line trajectories which represent trivial solutions to equation (4), i.e.

$$\begin{aligned} x&=0 \qquad \dot{y}=\mp\sqrt{2E} \\ y&=0 \qquad \dot{x}=\mp\sqrt{2E}. \end{aligned} \tag{7}$$

The two sets of straight-line orbits described by equations (7) and equation (5) represent two opposite extremes in the allowed behaviour of the particle with the Hamiltonian in equation (1). The unstable orbits given by equation (5) correspond to the most spatially confined motion whereas the orbits in equation (7) exhibits a completely delocalized behaviour with the particle moving at a constant velocity along the two troughs, where, of course, there is no force acting on the particle.

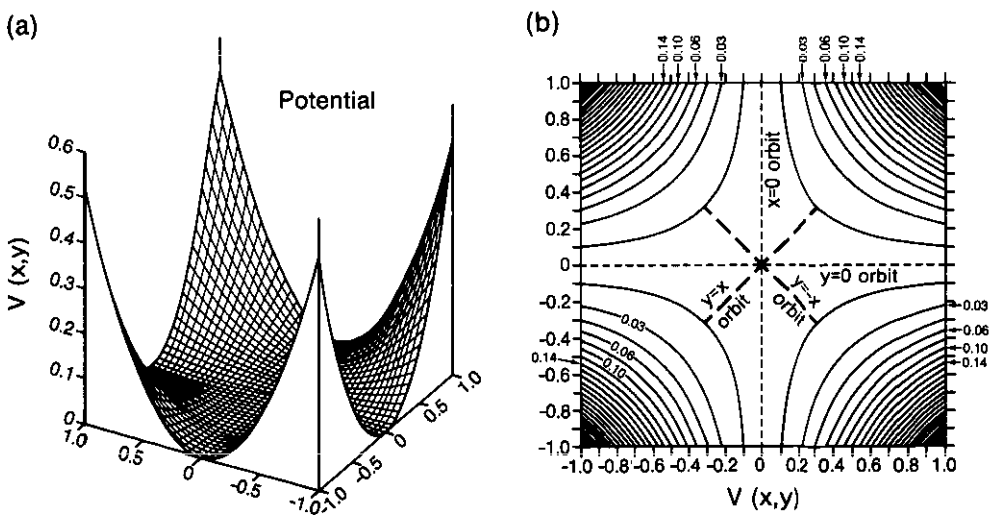

Figure 4. Plots of (a) the potential energy $V(x, y)=x^2y^2$ and (b) constant potential energy sections.

Plotting x versus t (or y versus t) provides another insight into how the unstable straight-line trajectories evolve under an infinitesimal perturbation. In figures 5(a–c), a comparison is made of the initial conditions $x_0 = -1.2$, -1.0 and -0.8, respectively. These correspond to the unstable straight-line orbit and its two quasi-periodic neighbours, one on each side. We see the emergence of a second period for both x and y as we move away from $x_0 = -1.0$. For lack of space only $x(t)$ plots are shown. However, we can obtain $y(t)$ plots from the $x(t)$ plots by changing x to $-y$ and similarly for the $\mathrm{d}y(t)/\mathrm{d}t$ versus t plots compared with $\mathrm{d}x(t)/\mathrm{d}t$ plots in figures 6(a–c). Finally, in this regard, the phase portrait in figures 7(a–c) illustrates, for $\mathrm{d}x/\mathrm{d}t$ versus x, how the initial unstable orbit characterized by

$$\dot{x}^2 = E - \tfrac{1}{2}x^4 \tag{8}$$

for $x_0 = -1$, becomes gradually distorted and modified for $x_0 = -0.8$ with step-like plateaux related to the development of a new periodicity. Equation (8) follows from

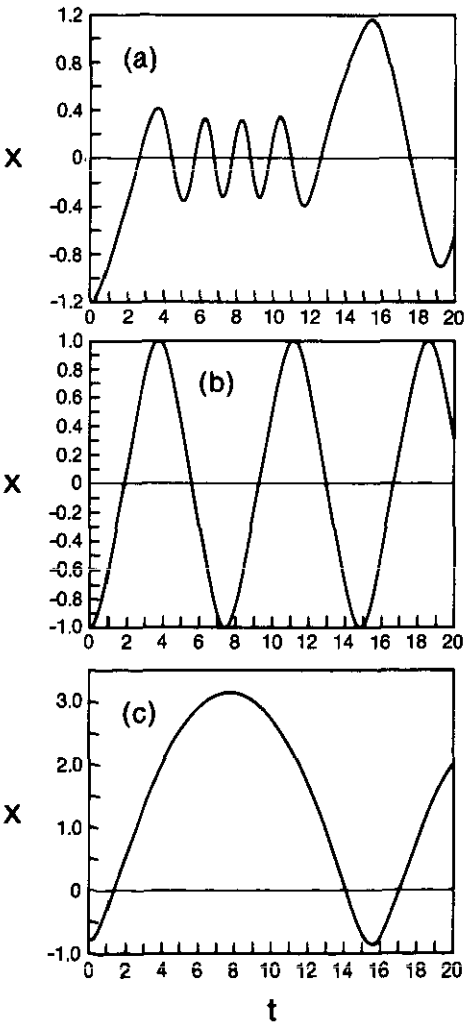

Figure 5. Plots of x versus t for $E = 0.5$ and (a) $x_0 = -1.2$, (b) $x_0 = -1.0$, (c) $x_0 = -0.8$.

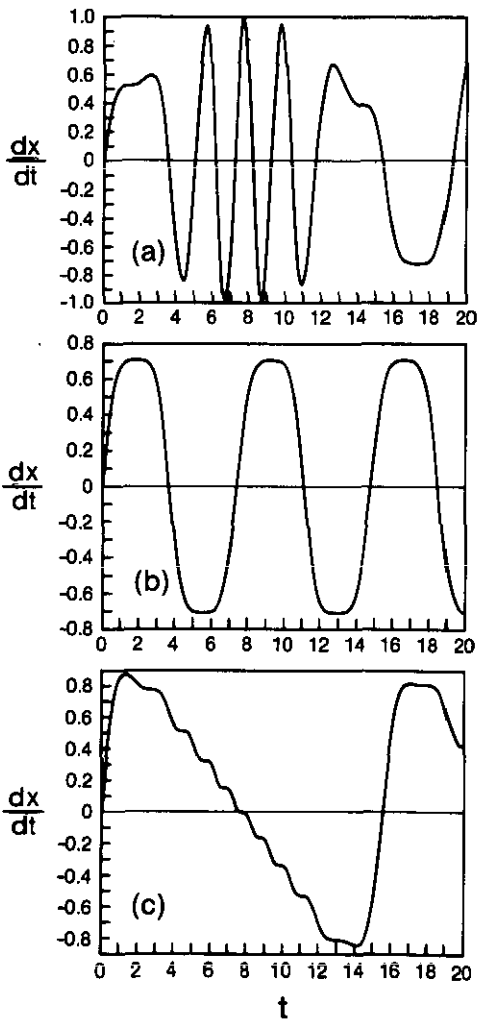

Figure 6. Plots of $\mathrm{d}x/\mathrm{d}t$ versus t for $E = 0.5$ and (a) $x_0 = -1.2$, (b) $x_0 = -1.0$, (c) $x_0 = -0.8$.

the conservation of energy condition applied to the $y = \mp x$ oribits. The other case, $x_0 = -1.2$, exhibits a different behaviour where the trajectory appears to be approaching an ellipse with its major axis rotated through 90° from the major axis in figure 6(b) for $x_0 = -1$.

It is perhaps of interest to provide approximate analytical forms for the beginning and ending portion of the quasi-periodic orbit in figure 1 so that once initial conditions are given the direction of launch or return direction is specified. For the orbit in figure 1 we have fitted straight lines to the initial and final parts of the trajectory for the range of x, $+1.8 \geqslant x \geqslant -1$. For the upper straight section the best fit is given by

$$y = -0.650\,038x + 0.760\,000 \tag{9}$$

whilst the lower section is best fitted by

$$y = +0.666\,519x - 0.648\,260. \tag{10}$$

This is illustrated graphically in figures 3(a) and 3(b) for equations (9) and (10), respectively.

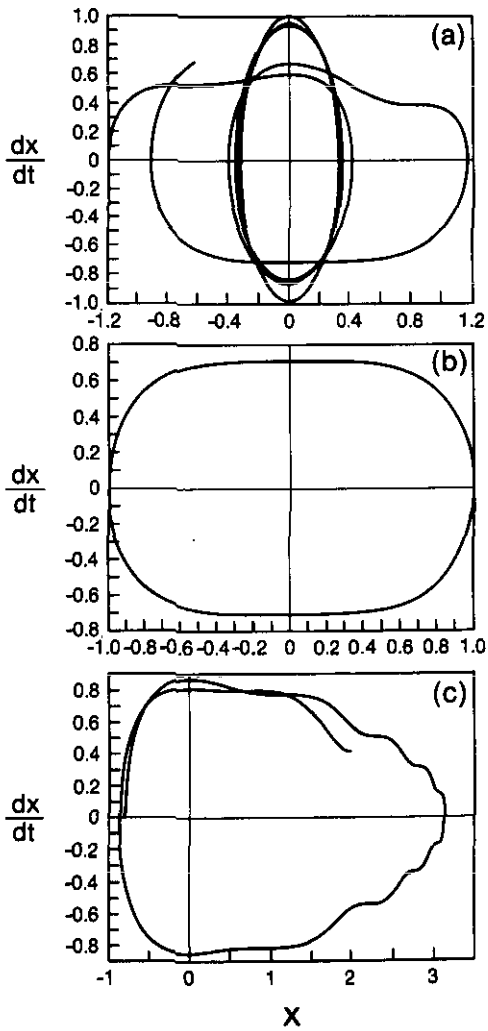

Figure 7. Surface of section plots in terms of dx/dt as a function of x for $E = 0.5$ and (a) $x_0 = -1.2$, (b) $x_0 = -1.0$, (c) $x_0 = -0.8$.

The computations described above were performed using a second-order Runge-Kutta method applied to the system of coupled equations in equation (4) on a given manifold of constant energy (in our case $E=0.5$ was chosen) using the step size of $h=0.005$. We have also used a fourth-order approach to check our calculations and the results remain the same. Each plot was constructed using approximately at least 400 points.

3. Perturbation calculations

An additional support for the numerical results of section 2 can be gained by perturbing the system of equations (4) with respect to the elliptic solution $x(t)$ in equation (5) and its counterpart $y=\mp x$. We seek solutions in the form

$$X(t)=x(t)+u(t) \qquad \text{and} \qquad Y(t)=y(t)+v(t) \tag{11}$$

where u and v are assumed to be small perturbations. We then obtain the coupled linear eigenvalue equations

$$\frac{d^2}{dt^2}\begin{pmatrix} v \\ u \end{pmatrix} = x^2\begin{pmatrix} -1 & -2 \\ -2 & -1 \end{pmatrix}\begin{pmatrix} v \\ u \end{pmatrix} \tag{12}$$

for the case $x=+y$ and

$$\frac{d^2}{dt^2}\begin{pmatrix} v \\ u \end{pmatrix} = x^2\begin{pmatrix} -1 & +2 \\ +2 & -1 \end{pmatrix}\begin{pmatrix} v \\ u \end{pmatrix} \tag{13}$$

when $x=-y$. Both cases can be readily diagonalized with the eigenfunctions

$$\phi_1=\frac{1}{\sqrt{2}}(v+u) \qquad \text{and} \qquad \phi_2=\frac{1}{\sqrt{2}}(v-u). \tag{14}$$

The corresponding eigenvalues are, respectively,

$$\begin{aligned} &\lambda_1=-3 \qquad \text{and} \qquad \lambda_2=+1 \qquad \text{for } x=+y \\ &\lambda_1=+1 \qquad \text{and} \qquad \lambda_2=-3 \qquad \text{for } x=-y. \end{aligned} \tag{15}$$

With $x(t)$ given by the elliptic function in equation (5) and the property (Byrd and Friedman 1971) that

$$\mathrm{sn}^2(\alpha t, k)+\mathrm{cn}^2(\alpha t, k)=1 \tag{16}$$

we can solve the problem completely with the aid of a monograph on special functions (Whittaker and Watson 1963). Substituting $x(t)$ from equation (5) into equations (12) and (13), after they have been diagonalized, results in a Lamé equation for the eigenfunctions, ϕ_1 and ϕ_2, of equation (11). Whenever these eigenfunctions correspond to positive eigenvalues the solutions take the form of scattered waves. However, a much more interesting set of solutions can be obtained for negative eigenvalues. The relevant Lamé equation takes the form

$$\frac{d^2\phi}{d\tau^2}=\{n(n+1)k^2\,\mathrm{sn}^2(\tau, k)+A\}\phi \tag{17}$$

where the scaled time variable is $\tau=t(2E)^{1/4}$ and $n=1$ for the eigenvalues of $\lambda=+1$ while $n=2$ for those with $\lambda=-3$. Note that $k^2=\frac{1}{2}$ and $A=+1$ and $A=-3$, respectively,

for the two cases above. The explicit analytical solutions take the form (Whittaker and Watson 1963)

$$\phi(\tau) = \prod_{r=1}^{n} \frac{H(\tau+\tau_r)}{\Theta H(\tau)} \exp\{-\tau Z(\tau_r)\} \tag{18}$$

where Θ and Z are the Riemann theta and zeta functions, respectively, while H is Jacobi's eta function. The constant values τ_r satisfy a specific set of equations which can be deduced from the original source. Note also that, for our case for $\lambda = +1$ only one term is present in the product in equation (18) ($n = 1$) while the other case is the product of only two factors. Thus, the cases under consideration are the two simplest possibilities for the Lamé eigenvalue problem. The functions $\phi(\tau)$ can be doubly periodic which would physically imply a periodic envelope with internal oscillations around the centres of the potential minima in equation (17). Having solved the problem for the 'diagonalized' eigenfunctions ϕ, we can now revert back to the original eigenfunctions u and v which will now be composed of, in general, two contributions. One of these will be a scattered wave solution of the Lamé equation (for positive eigenvalues) which modifies the other component that has two periods. Note that the minus sign appearing in equation (17) for positive eigenvalues can be absorbed in k^2 yielding an imaginary value of the Jacobi modulus. This explains the scattered wave nature of this type of solution.

It is also possible to derive a second-order differential equation for $y = f(x)$ which describes the particle's *regular analytical trajectories*. If primes denote differentiation with respect to x then clearly

$$\dot{y} = f'\dot{x}. \tag{19}$$

Hence, differentiating equation (19) again with respect to time and using the equations of motion in equation (4), we find that

$$f''(\dot{x})^2 - f'f^2x = -fx^2. \tag{20}$$

However, for a fixed energy E, from the first integral, we have

$$2E = (\dot{x})^2 + (\dot{y})^2 + x^2y^2 = (\dot{x})^2 + (f')^2(\dot{x})^2 + x^2f^2. \tag{21}$$

Eliminating $(\dot{x})^2$ between equations (20) and (21) then provides the equation of the trajectories as

$$f''(2E - x^2f^2) = xf(1+(f')^2)(-x+ff'). \tag{22}$$

Two solutions of equation (22) are evident, namely those corresponding to the unstable orbits $f(x) = \mp x$, when $x(t)$ is described by the elliptic function in equation (5). It is interesting to note that for small values of f, equation (22) reduces to

$$f'' = \frac{-x^2}{2E} f. \tag{23}$$

This is a Bessel function equation with one solution of the form

$$f = \sqrt{x}\, J_{1/4}\left(\sqrt{\frac{2}{E}}\,\frac{x^2}{4}\right) \tag{24}$$

and will exhibit damped oscillatory behaviour near the axes. Consequently, we have found approximate expressions for the intersection points of the trajectory with the x and y axes represented by the zeros of the Bessel function in equation (24).

4. Comments on the properties of orbits

In the context of physical applications to the confinement problems of plasma in the presence of a magnetic field given by equation (3) it is of interest to explore the existence and properties of the farthermost points (from the origin of the coordinate system) on a given trajectory. Such a point, at (x_F, y_F), is characterized by an infinite or at least very large gradient, i.e. $f' = dy/dx \to \infty$, and by both velocity components becoming vanishingly small, i.e. $\dot{x}, \dot{y} \to 0$. Using equation (22) and neglecting the terms that become insignificant in the circumstances we arrive at the following approximate equation

$$(2E - x_F^2 y_F^2) f'' \simeq 2(f')^3 x_F y_F^2 \tag{25}$$

valid for $x \simeq x_F$ and $y \simeq y_F$, i.e. close to the farthest point.

A few comments are in order regarding equation (25) and the assumptions made in deriving it. First, due to the 90° rotational symmetry of the Hamiltonian, if an orbit has $f' = \infty$ at its farthest point from the origin, then another, rotated orbit must have $f' = 0$ at this point. However, we consider here only the former case. We also exclude the special cases of the $y = \pm x$ orbits for which $f' = \pm 1$ at all times. Furthermore, the condition $\dot{r} = 0$ allows two possibilities $\dot{x} = 0$ or $f' = -x/y$. Since $f' = dy/dx = \dot{y}/\dot{x}$, the first possibility does indeed give $f' = \pm\infty$ as long as $\dot{y} \neq 0$. In fact, on crossing the x-axis with $\dot{x} \neq 0$ we obtain $\dot{y} = \pm\sqrt{2E}$. However, if $\dot{x} \neq 0$, then we must have $f' = -x/y$ even if $\dot{x}$ is very small. Therefore, it is very important to determine whether $\dot{x}$ is exactly zero or just small. In the case when both $\dot{x}$ and $\dot{y}$ are negligibly small we obtain from energy conservation for the Hamiltonian of equation (1) that

$$y_F \simeq \pm\sqrt{2E}/x_F. \tag{26}$$

Between the points with $\dot{x} = 0$, $y = 0$ and $x = x_F$ the trajectory is nearly a straight vertical line, so we can approximate $x \simeq x_F$, $\dot{x} = 0$ and solve the equation of motion for $y = y(t)$. This gives $y = y_F^0 \sin(\omega t)$ with $y_F^0 = \sqrt{2E}/x_F$ being the amplitude of vertical motion and $\omega = x_F$ its frequency. Increasing the position of x_F results in decreasing the amplitude y_F^0. We have checked the relation given in equation (26) for our orbit in figure 1 where

$$x_F = 3.1328 \qquad y_F = 0.3184 \qquad E = 0.5. \tag{27}$$

The result of our comparison of these numbers with equation (26) is excellent as can be readily verified by the reader. Obviously, corresponding orbits at higher energies will be characterized by end points whose coordinates will be related to those above for having $E = 0.5$ through a simple scaling by a $\sqrt{2E}$ factor. Another comment worth making is that equation (26) implies no obvious limit on the magnitude of x_F for a fixed value of energy E. This is in agreement with the straight-line orbits along the troughs given by equation (7).

5. Conclusions

In summary, we have provided an analysis of motion close to the straight-line orbits of the x^2y^2 potential. The tools we have employed were both analytical and numerical. It was shown that quasi-periodic orbits close to the unstable straight-line orbits can be understood in terms of infinitesimally small perturbations applied to special types of analytical solutions. A particularly interesting result has been derived for the end

points of any low-energy orbits and we believe that it can be of practical value in plasma confinement studies.

We also believe that we have demonstrated, not only a physical reason for the observed behaviour of the system but also an intriguing insight has been obtained into an analytical approach to a partially chaotic problem.

Acknowledgments

This project is supported by grants from NSERC (Canada) and NATO. The authors express their gratitude to Dr G Rowlands of the University of Warwick for drawing their attention to this problem.

References

Biswas D, Azam M, Lawande Q V and Lawande S V 1992 *J. Phys. A: Math. Gen.* **25** L297
Byrd P F and Friedman M D 1971 *Handbook of Elliptic Integrals for Engineers and Scientists* (Berlin: Springer)
Carnegie A and Percival I C 1984 *J. Phys. A: Math. Gen.* **17** 801
Chang S-J 1984 *Phys. Rev.* D **29** 259
Chirikov B V and Shepelyonsky D L 1981 *JETP Lett.* **34** 163
Dahlqvist P and Russberg G 1990 *Phys. Rev. Lett.* **65** 2837
Feingold M, Moiseyev N and Peres A 1985 *Chem. Phys. Lett.* **117** 344
Martens C C, Waterland R L and Reinhardt W P 1989 *J. Chem. Phys.* **90** 2328
Matanyan S G, Savvidy G K and Ter-Arutyunan-Savvidy N G 1981 *Sov. Phys.-JETP* **53** 421
Murphy G M 1960 *Ordinary Differential Equations and Their Solutions* (Princeton, NJ: Van Nostrand)
Nikolaevskii E S and Shur L N 1982 *JETP Lett.* **36** 218
Savvidy G K 1983 *Phys. Lett.* **130B** 303
—— 1984 *Nucl. Phys.* B **246** 302
Sohos G, Bountis T and Polymilis H 1989 *Nuovo Cimento* B **104** 339
Steeb W H, Villet C M and Kunick A 1985 *J. Phys. A: Math. Gen.* **18** 3269
Whittaker E T and Watson G N 1963 *A Course of Modern Analysis* (Cambridge: Cambridge University Press)